Online Journal of Space Communication

Volume 1
Issue 2 *NASA's Advanced Communications Technology Satellite [ACTS] (Fall 2002)*

Article 8

September 2002

ACTS Propagation Experiment: Experiment Design, Calibration, and Data Preparation and Archival

Robert K. Crane

Xuhe Wang

D. B. Westenhaver

Wolfhard J. Vogel

ACTS Propagation Experiment: Experiment Design, Calibration, and Data Preparation and Archival

ROBERT K. CRANE, FELLOW, IEEE, XUHE WANG, D. B. WESTENHAVER, AND WOLFHARD J. VOGEL, FELLOW, IEEE

The National Aeronautics and Space Administration Advanced Communications Technology Satellite (ACTS) propagation experiment was designed to obtain slant-path attenuation statistics for locations within the United States and Canada for use in the design of low-margin Ka-band satellite communication systems. Experimenters at seven different locations have collected propagation data for more than two years. The propagation terminals used for the experiment were identical. A single preprocessing program was used by the experimenters to provide for automatic calibration, generation of attenuation histograms, and data archival. In this paper, the calibration procedures are described and estimates given for measurement accuracy.

ACTS provided beacons at 20.2 and 27.5 GHz for use in making attenuation measurements. In addition to the beacon receivers, each ACTS propagation terminal has two total power radiometers with center frequencies at the beacon frequencies. The radiometers are used to establish the beacon signal reference levels needed for calculating beacon attenuation values. For the combined radiometer and beacon measurement system, the attenuation measurement error was less than a maximum of 1.0 dB and was generally less than 0.3 dB. The dynamic range for attenuation measurement varied from site to site depending on location relative to the peak of the satellite beacon antenna pattern. For locations within the continental United States, the dynamic range was better than 20 dB.

Keywords**—** *Attenuation, attenuation measurement, microwave radio propagation meteorological factors, microwave radiometry, millimeter wave communication, millimeter wave radio propagation meteorological factors, rain, satellite communication.*

I. INTRODUCTION

The National Aeronautics and Space Administration (NASA) Advanced Communications Technology Satellite (ACTS) propagation experiment was designed to obtain slant-path beacon attenuation statistics at Ka-band frequencies (20.2 and 27.5 GHz) [1], [2]. These measurements were to be made in different rain-rate climate regions (or zones) within the United States and Canada to provide additional information for the design of low-margin satellite communication systems. At the time of this writing, ACTS was still operating and over three years of propagation data had been collected. The papers in this special issue of the PROCEEDINGS summarize the results from the first two years of propagation observations.

A number of beacon attenuation measurements were made previously in the United States, Europe, and Japan [3]. In the 19–31 GHz frequency range, the COMSTAR measurement program in the late 1970's in the United States produced 27 path years of observations [4]. The recent OLYMPUS propagation measurement program (OPEX) conducted in Europe produced 12 path years of data in the same frequency range [5] (plus 11 additional path years if 11 months of observations is considered a year). For the COMSTAR measurements, 21 of the path years of observations were made in the same rain climate zone and only three climate zones within the United States were sampled. The 12 path years of data from OPEX were obtained in a total of five climate zones but five of the path years were from a single climate zone. From the two years of observations summarized in this special issue, an additional 26 path years of observations from six climate zones have been added to the propagation data base. Three of the climate zones had not been sampled before at these frequencies.

The ACTS propagation experiment was designed to acquire additional attenuation statistics for use in propagation model development and verification. The goal is to provide information on propagation phenomena that affect low-margin satellite communication systems operating at Ka-band frequencies. At these frequencies, significant path attenuation can be produced by rain, clouds, and atmo-

Manuscript received September 1, 1996; revised November 1, 1996.

R. K. Crane is with the University of Oklahoma, School of Meteorology, Norman, OK 73072 USA (e-mail: bcrane@ou.edu).

X. Wang is with the University of Oklahoma, Norman, OK 73019-0628 USA (e-mail: xwang@tornado.gcn.uoknor.edu).

D. B. Westenhaver is with Westenhaver Wizard Works, Inc., Stone Mountain, GA 30087 USA (e-mail: wwwinc@crl.com).

W. J. Vogel is with the University of Texas, Electrical Engineering Research Laboratory, Austin, TX 78758 USA (e-mail: Wolf.Vogel@mail.utexas.edu).

Publisher Item Identifier S 0018-9219(97)04654-9.

spheric gases (oxygen and water vapor). Rapid variations in signal level can be produced by changes in the rain or clouds and by turbulent variations in the index of refraction along the path. Not all the changes in signal level are caused by the propagation medium. Water on the surface of the antenna or on an antenna feed window can also produce signal attenuation. The receiver system was designed to observe the changes in received signal level due to all causes. The data recording and processing system was designed to provide sufficient data to analysts to identify the phenomena responsible for the observed signal level changes.

Satellite communication system designers need to know the expected probability distribution for signal level changes. Prior observations have shown that rain can reduce the signal level by more than 30 dB for frequencies in the 20–30 GHz range [6]. In the presence of such a fade, communications may not be possible. Schemes for the use of uplink power control, coding, or site diversity have been proposed to overcome the effect of a deep fade [7]–[9]. How often will they be required and how well will they work? In the absence of a mitigation scheme, how often will a communication link be unavailable for use? These are questions that need to be answered. The information required by the system designer is contained in the probability distribution for path attenuation on a single path, in the joint distribution of attenuation on spatially separated paths for site diversity, in the joint distribution of attenuation at different frequencies for uplink power control, and in the joint distribution of attenuation at closely spaced time intervals for coding.

The ACTS propagation experiment was designed to provide estimates of the probability distributions for path attenuation on single paths, the joint distributions for time intervals separated by 1/20 s or longer, and the joint distributions at two frequencies, 20.2 and 27.5 GHz. Data from one of the ACTS propagation experiment sites has been used to investigate site diversity [10].

II. Experiment Design

ACTS carries beacons at 20.2 and 27.5 GHz for use in the maintenance and control of the ACTS communications networks. The beacons can also be used for propagation experiments. NASA provided for the design and construction of seven identical propagation terminals for use by experimenters in the collection of propagation data [11].

The characteristics of the propagation terminal are given in Table 1. The terminal equipment included computer-controlled beacon receivers and collocated total power radiometers operating at the beacon frequencies. The receivers were designed for continuous unattended operation with periodic calibration of the total power radiometers. The data were recorded for postprocessing analysis and archival. Because the receiver systems were identical, a single preprocessing program for first-level postprocessing analysis was used by all the experimenters.

The basic recording mode collected beacon and radiometer data for a propagation terminal continuously at one sample per second. These data were combined with a time stamp, meteorological observations, and receiver status information and stored in daily output files. The unprocessed (or raw) daily data files were input to the preprocessing program, which performed the calibration functions, generated attenuation histograms, and prepared one-minute average and standard deviation estimates for beacon signal level, beacon attenuation, radiometer-derived sky brightness temperature, and radiometer-derived attenuation. The preprocessing program also extracted the meteorological, status, and calibration control information from the raw data files. The calibrated one-second attenuation estimates were output to daily preprocessed data files together with time, surface weather, and status data. The one-minute average samples were also output to daily files for spreadsheet analysis. The histograms were output to monthly files for postanalysis.

Table 1 ACTS Propagation Terminal and Preprocessing Program Characteristics

Antenna	1.2 m offset reflector
Radiometer	Total power 100 MHz bandwidth (including image) Periodic noise injection calibration every 15 minutes 1500 K receiver noise temperature (nominal) 6 K rms measurement accuracy for 1 second integration time 4 K rms measurement error relative to theoretical values obtained from radiosonde balloon data < 0.3 dB rms error in estimated attenuation under clear sky conditions
Beacon Receiver	Digital using cascaded FFTs Frequency tracking 1 Hz detection bandwidth < 3 s to reacquire after loss of signal 0.1 dB rms measurement accuracy 20 dB dynamic range (nominal)
Data Collection	1 sample per second recording standard 20 sample per second recording mode available Time (year, month, day, hour, minute, second) Beacon signal level (dB arbitrary reference) Radiometer voltage Receiver system status Surface weather at the terminal
Preprocessing	Automated beacon reference level determination < 0.3 dB rms error in estimated attenuation Fade duration and interfade interval determination Attenuation histogram generation Output of calibrated attenuation data for time series analysis Output of one-minute averages for spreadsheet analysis

The second-by-second daily attenuation time series are available from the ACTS propagation archives at the Electrical Engineering Research Laboratory, University of Texas [12] for use by anyone interested in their analysis or by engineers interested in simulating the effects of attenuation on their system design. The preprocessed data are available from all the sites for the first two years of observations on a set of four CD-ROM's. The preprocessing program is also supplied on one of the discs and can be used to regenerate the minute-by-minute summary files for any day and any site. The daily histograms are also available for use in summarizing the data or as an index for looking at the minute-by-minute time series. These data can be used by other investigators to explore different statistics.

The propagation terminals were provided with meteorological sensors to record the temperature, pressure, relative humidity, wind speed, wind direction, and rain rate continuously at the surface. These data were averaged for one minute and were sampled and recorded in the same files as the beacon and radiometer data. The preprocessing program used the surface data to transform the radiometer observations to attenuation estimates and to record rain-intensity statistics.

The data-recording system was designed to collect status data on the important components in the beacon and radiometer systems. These data were sampled once each minute. The signals needed for radiometer calibration were generated once each 15-min period and recorded. The preprocessing program performed the calibrations and generated the attenuation estimates.

III. Statistical Considerations

The cumulative distributions of measured path attenuation change from day to day, month to month, and year to year [13]. The observed cumulative distribution (the empirical distribution function or EDF) for a single month or year does not provide a good estimate of the underlying probability distribution for the rain attenuation process because of the large apparent variability in the EDF's observed for a single path and frequency over a period of a few years. A minimum of about six years of observations is required to produce a stable distribution estimate, i.e., a distribution with a statistical error of 10% in dB at a fixed value of probability. Five years of measurements are required to produce a distribution estimate with an 11% uncertainty. To date, only three locations worldwide have produced five years or more of observations. The ACTS propagation experiment should more than triple the amount of data available.

Even for the ACTS propagation experiment, sufficient data to provide a precise estimate of the probability distribution for attenuation on an experiment path cannot be collected over the lifetime of the satellite. Reference must be made to the 122 path years of single-year beacon data in the database of the radiocommunications sector of the International Telecommunications Union (ITU-R) [3] or the 65 path years of beacon data in the University of Oklahoma data base [14] to produce model distributions with parameters that may be estimated from the ACTS observations. In the end, it is the model that is important because only a model is useful for the prediction of the attenuation distribution for another path. The ACTS propagation experiment should be viewed as an experiment in model validation and model parameter estimation, not as an experiment to produce a probability distribution.

The expected deviation of a single-year EDF from the actual probability distribution for that site and path is outside the range of −21% to +26% of the attenuation value in dB at a fixed probability value for one year in three (33% of the years of observation) based on a simple model and all the prior observations in the archives [13]. The differences between most prediction models are generally less than the expected year-to-year variations. Fig. 1 presents the distribution predictions of four different models for the Norman, OK, experiment site for a frequency of 27.5 GHz. Two types of models are presented: the ITU-R model [15] and the Dissanayake, Allnutt, and Haidara (DAH) models [16], which summarize the data in the ITU-R archives and the Crane–Global [17] and Crane–Two Component [9] models, which are based on a physical model for attenuation by rain and statistical analyses of rain gauge and weather radar data.

The upper and lower bounds presented in the figure encompass the expected range for five-year average EDF's for 90% of the five-year periods with observations if the Crane–Two Component model is exact. The expected range is logarithmic and applies for all the models in the figure (when plotted on a logarithmic scale). For measured EDF's to be useful in model validation, the 90% uncertainty in an EDF should be smaller than the differences between the models. Using five years of data, the EDF should lie between the upper and lower bound curves (for 90% of the experiments) about a model prediction to be in agreement with the model. With five years of data and a 10-dB dynamic range, the difference between agreement with the Two Component model and the DAH model could be clearly established but the difference between the Global model and the Two Component model might not be established. With a 20-dB dynamic range, each of the models displayed in Fig. 1 could be tested and the best model could be established.

In addition to the requirement for a long observation period to reduce statistical uncertainties, other measurement requirements must also be met if the observations are to be used for model validation: 1) a wide, 0–20 dB, dynamic range for the measurement of attenuation, 2) a measurement accuracy of better than 0.5 dB, and 3) continuous observations with less than a 10% loss in data. These three requirements were used as specifications for the propagation terminal design [11].

A wide dynamic range is needed to provide valid measurements at both high and low attenuation levels. Low attenuation levels must be observed because of interest in low-margin systems; high attenuation levels must be observed so the EDF's can be used to verify predictions based on models developed from lower frequency observations. The current ITU-R and DAH models build their predictions on estimates of the attenuation to be observed 0.01% of a year. At a central U.S. site such as in Norman, OK, at 0.01% of a year, the ITU-R model attenuation prediction at 27.5 GHz is 16 dB if the ITU-R model is used, and over 43 dB if the Crane–Global model is used. At this frequency, measurements are not possible at 0.01% of a year but may be made at 0.1% of a year. Even at this probability value, a wide dynamic range is needed.

The acceptable measurement error was specified to be 0.5 dB. If the maximum signal loss on a low-margin system is 5 dB for acceptable communication, a measurement uncertainty of 3 dB is not useful. For such a system, a 0.3-dB uncertainty would be preferred. The specification for system design was a typical error of 0.5 dB and a measurement resolution of 0.1 dB. With this measurement accuracy, the

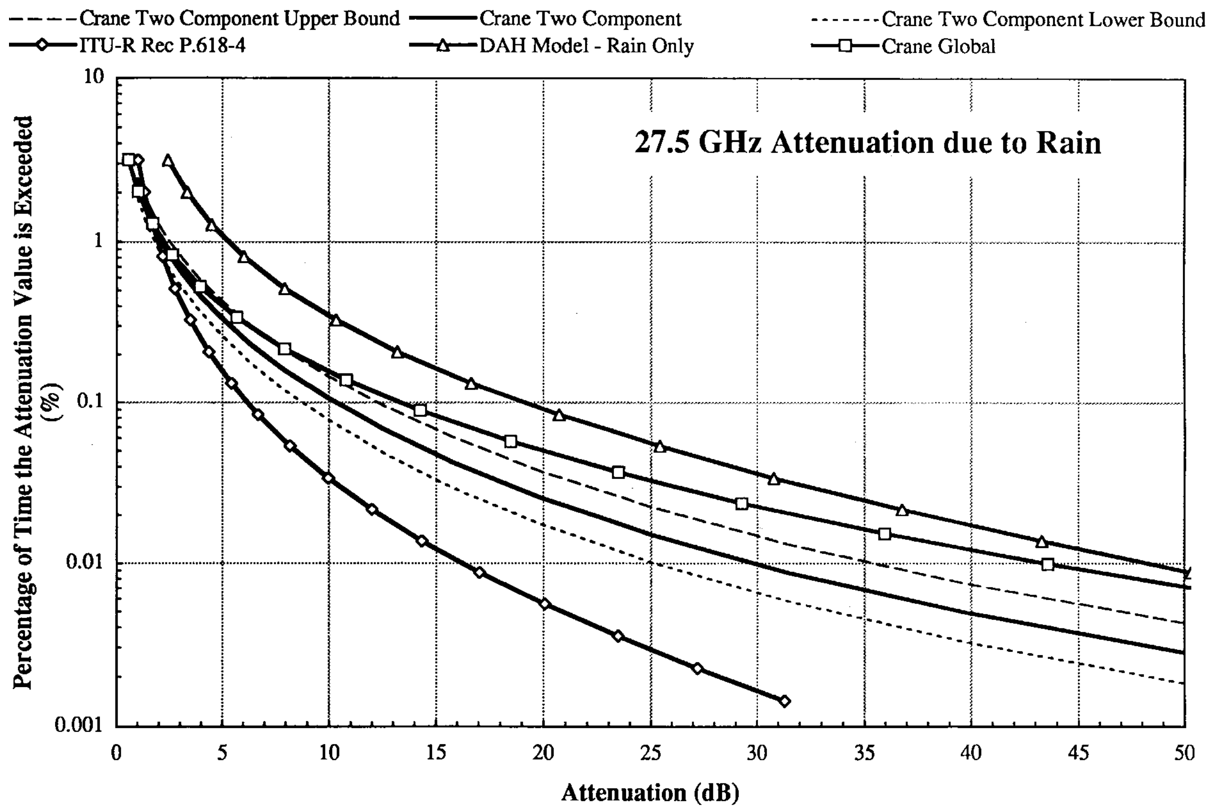

Fig. 1. Attenuation model predictions for five years of observation at the ACTS propagation experiment site in Norman, OK.

best model could be selected if the measurement period is of sufficient length to effect a significant reduction in the statistical uncertainties in the distribution estimates. The light dashed lines in Fig. 1 provide the expected upper and lower bounds at a 0.1 significance level if a full five years of observations are available.

The long-term observations will provide valid probability distribution estimates only if a reasonably complete set of observations is made. If the equipment is only operable half the time and not when it is raining, no valid distribution estimate is possible. If it is operable 90% of the time and equipment failure occurrences are independent of the rain occurrences, then the uncertainty bounds are only slightly larger than shown in Fig. 1. The specification was for better than 90% equipment availability and independence between equipment failures and rain occurrences. To provide the latter, extensive equipment grounding and uninterruptable power supplies were used at each site to guard against the loss of operations during thundershowers.

IV. Calibration

The specification of an attenuation measurement error of less than 0.5 dB demands nearly continuous calibration of the radiometer channels and continuous modeling and estimation of the power transmitted by the satellite beacons. The radiometer observations were used to determine the path attenuation during periods with attenuation values less than 4.0 dB and a one-minute standard deviation of the beacon signal level of less than an elevation-angle-dependent threshold value (0.12 dB at a 49° elevation angle). These limits were set to maximize the accuracy of the radiometer estimates of attenuation. The radiometer and beacon measurements of attenuation then should be identical. The attenuation estimated from the radiometer is combined with the simultaneously observed beacon signal level to correct for path attenuation between the satellite and the propagation terminal. The combined beacon signal level plus radiometer-estimated attenuation value should be the reference level for the estimation of beacon attenuation. During periods with significant attenuation (greater than about 6 dB), the radiometer will not provide a satisfactory estimate of the attenuation value and another scheme is necessary to provide a reference level.

A. Beacon Calibration

Predictions of the unattenuated beacon signal level were used to provide a reference level during periods with high attenuation. The prediction scheme is based on the use of a fourth-order harmonic fit to the diurnal variations of the unattenuated beacon signal levels observed either on the prior day or, if the data for the day of interest has been processed before, for the current day. The deviations of the observations from the harmonic predictions for each hour are then used in a least-squares, second-order harmonic corrector with autoregressive coefficients. The predictor has a time constant of three hours and decays gracefully to the best-fit reference level for the prior (or current) day. The resultant reference level estimator tracks the reference level

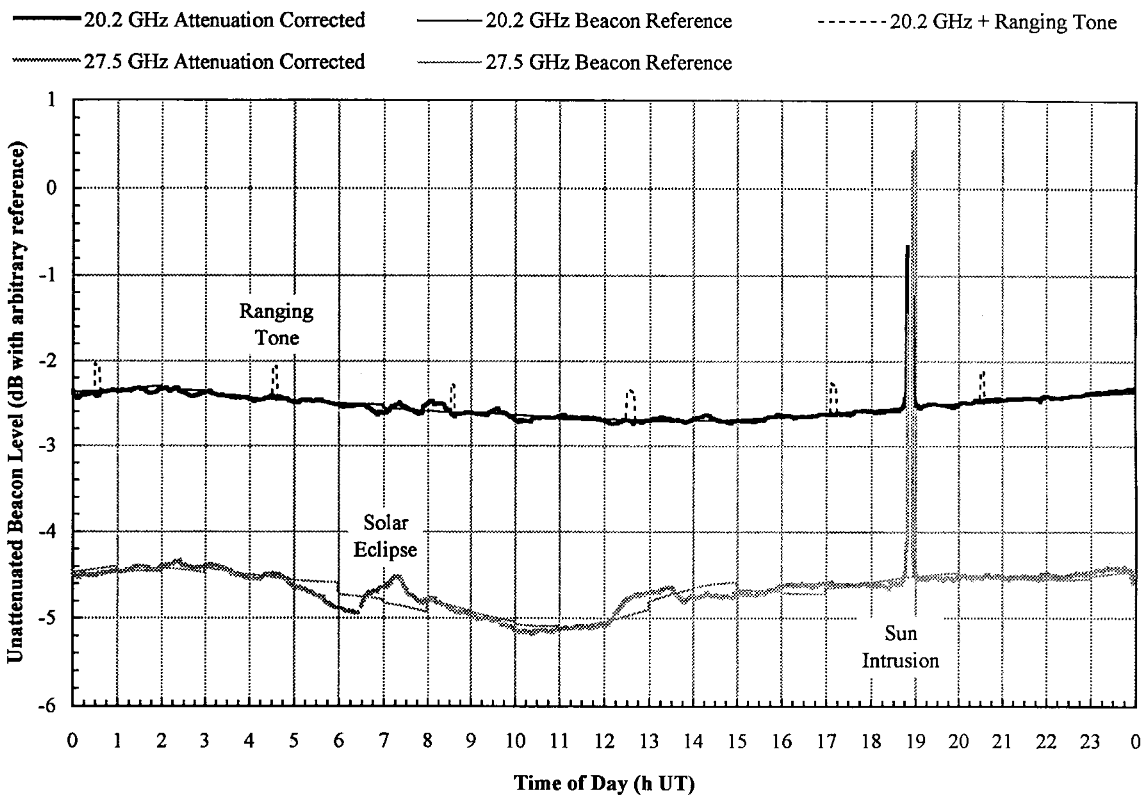

Fig. 2. Unattenuated beacon signal level estimates, March 6, 1995, Norman, OK.

observations with a root mean square (rms) error of less than 0.1 dB during undisturbed conditions. It provides valid reference-level estimates during periods with significant attenuation (> 4 dB or beacon levels with high standard deviation values).

The major problem with the reference level estimation scheme occurs during solar eclipse periods at the satellite. The solar eclipses occur for about a month during the spring and a month in the fall. The thermal stress on the satellite antenna caused by the transition from sunlight to darkness and the satellite electrical power level changes due to the switch from a solar panel to battery power create changes in beacon frequency and rapid changes in the radiated power toward a propagation terminal. These changes are not repeatable from one day to the next and cannot be tracked by an algorithm designed to provide smoothed reference levels during rain storms. The operation of the reference level estimation scheme for a quiet period, solar eclipse, time with rain, and time with a sun intrusion (in the main lobe of the propagation terminal antenna pattern) are shown in Figs. 2 and 3. Sun intrusions affect only the radiometer channels. They occur during one week each spring and fall. In each figure, the estimated unattenuated beacon power level and the smoothed reference levels are shown for each beacon frequency. The small discontinuities in reference level at the start of each hour are caused by calculating the autoregressive coefficients only once per hour. The 20.2-GHz beacon changes modulation state for periods of about 15 min to facilitate satellite tracking by the master control station. The result is the signal level increases (called ranging tones) indicated by the dashed curves. The ranging tones were removed by the preprocessing program.

During quiet times, the unattenuated beacon power levels were within 0.04 dB (rms difference) of the smoothed reference level estimates at 20.2 GHz and within 0.08-dB rms at 27.5 GHz. The sun intrusion was automatically detected and removed from the reference level estimation process. The solar eclipse produced deviations of less than 0.2 dB at 20.2 GHz and 0.4 dB at 27.5 GHz. On March 7, 1995 (Fig. 3), rain occurred during the time of the solar eclipse. The predicted reference level is still available for the estimation of beacon attenuation. The maximum error during the rain interval is less than 0.4 dB. The larger excursions of the unattenuated beacon power levels arise from errors in using radiometer observations to estimate beacon attenuation when the attenuation value is more than 4 dB and the standard deviation is larger than 0.1 dB in rain. These unattenuated beacon levels were not used in the determination of the reference level or in the estimation of new coefficients for reference-level prediction. The antenna reflector may also have been wet during the rain event. Because the attenuation produced by a wet antenna equally affects both the beacon and radiometer systems, the calibration procedure works even in the presence of wet antenna surfaces.

The radiometer can usually provide a good estimate of the beacon attenuation except during the onset or cessation of a rain event, when the spatial distribution of rain along the path differs from the distribution assumed for times within a rain event or when the attenuation is more than

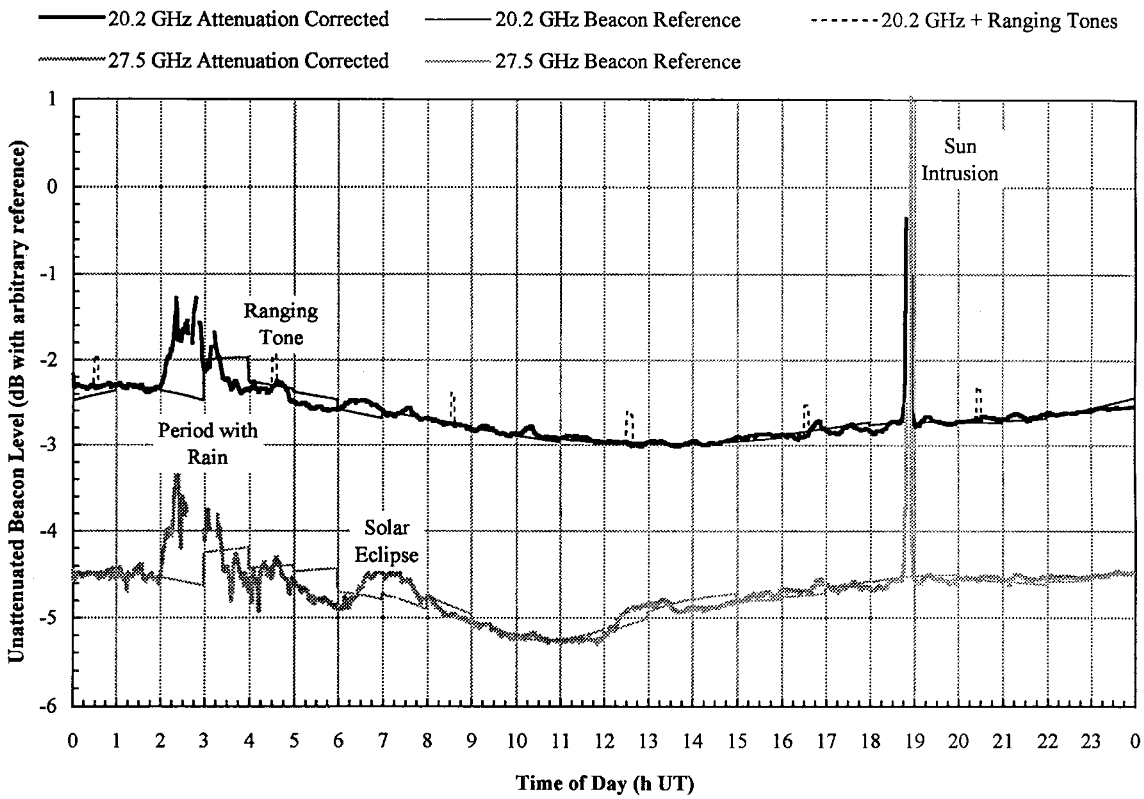

Fig. 3. Unattenuated beacon signal level estimates, March 7, 1995, Norman, OK.

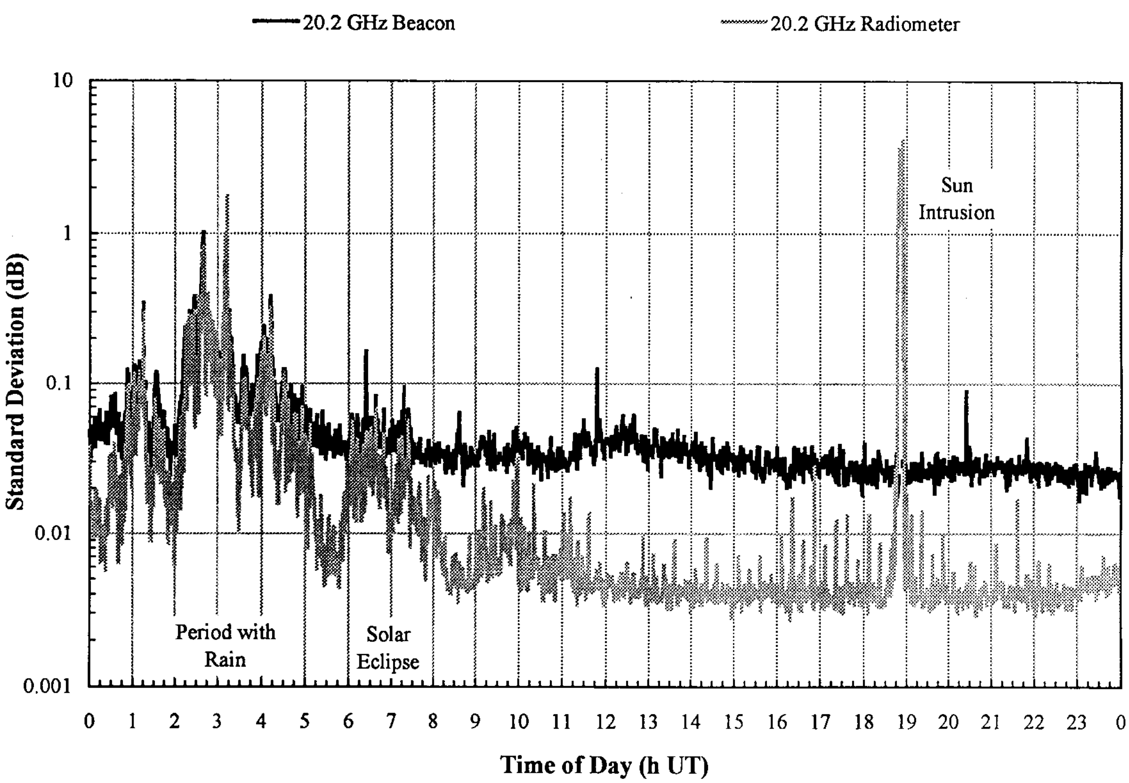

Fig. 4. Beacon and radiometer attenuation standard deviation estimates at 20.2 GHz, March 7, 1995, Norman, OK.

4 dB in the rain event. Times when the standard deviation of the beacon signal level is higher than expected are often indicative of attenuation by rain. Fig. 4 shows the standard deviation values at 20.2 GHz for March 7. Fig. 5 shows the attenuation values at 20.2 GHz for the same date. During periods with attenuation greater than 4 dB and standard

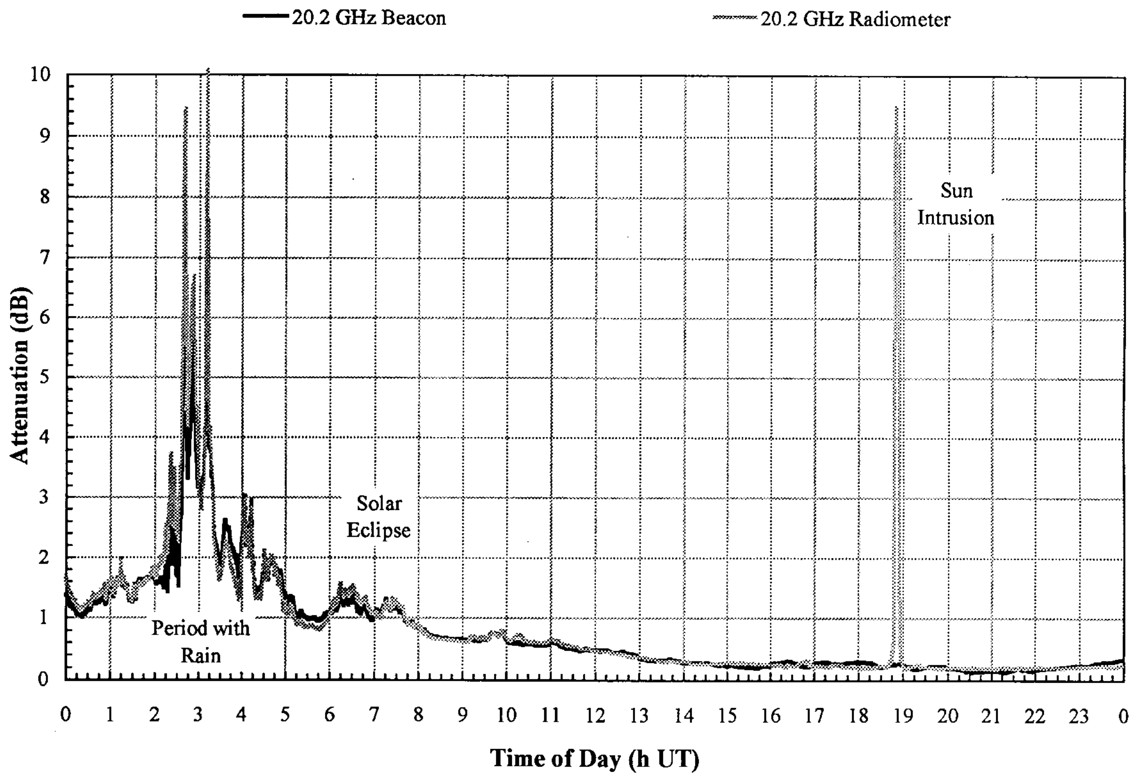

Fig. 5. Beacon and radiometer attenuation estimates at 20.2 GHz, March 7, 1995, Norman, OK.

deviations greater than 0.12 dB, the radiometer data were not used to update the beacon reference level estimation parameters. During the quiet times after 8:00 h universal time (UT), the radiometer and beacon attenuation values differ by less than 0.2 dB and the standard deviation of the attenuation estimates from the radiometer are nearly an order of magnitude smaller than the standard deviations of the beacon signal level. During the rain event, 0:00–8:00 h UT, the radiometer and beacon attenuation values differ by less than 0.3 dB in the periods between showers when the attenuation is less than 2 dB (see also Fig. 7). The use of the reference-level prediction provides an estimate of beacon attenuation that agrees closely with the radiometer estimates even in the times between showers and, by continuity, provides a good reference-level estimate when the radiometer cannot provide a valid attenuation estimate.

B. Radiometer Calibration

The radiometer provides the low attenuation reference for the estimation of beacon attenuation. The digital beacon receiver provides the precise measurement of the relative changes in beacon level for attenuation values greater than 4 dB that extend the dynamic range of the radiometer observations. The radiometer provides the reference or base for the estimation of attenuation. To complete the system calibration, the total power radiometer must be considered. Wide-bandwidth, high-gain total power radiometer systems are prone to slow changes in time. To provide a stable system, known power level changes are inserted into the radiometer receiver and the receiver output is corrected to match these changes. The change in noise temperature T measured by the radiometer is linearly related to the radiometer output voltage V by

$$T = aV + b' - T_R = aV + b$$

where T_R is the unknown slowly varying receiver noise temperature and a, b' are slowly varying constants related to the electronic circuits between the radiometer detector and the analog–digital converter used to record the data. Two levels of noise are injected to determine the two constants. The two known power levels are established by switching the receiver from the antenna to a dummy load and inserting additional noise power from a noise diode. The change in power caused by the noise diode is known and the temperature of the dummy load is controlled and continuously monitored. The step changes in radiometer-estimated attenuation values caused by changes in the calibration constants at calibration time are generally less than 0.1 dB and usually cannot be detected (see Fig. 11). The radiometer calibrations are repeated at 15-min intervals. Each calibration takes 20 s to complete.

C. Overall Radiometer System Calibration

The radiometer is connected to the antenna via a waveguide switch. The power detected by the radiometer is collected from the noise power incident on the antenna and the noise power generated by losses in the switch and waveguide. The power incident on the antenna arises from atmospheric emission by rain, clouds, and gases in the antenna main beam and sidelobes and from surface emission from the ground, buildings, and the structure supporting the antenna. The noise detected by the radiometer is related to the sky brightness temperature T_B by

$$T = c(\eta T_B + (1-\eta)T_S) + dT_W + fe^{-\left(\frac{(P_b - P_o)}{4.343}\right)}$$

where c, η, d, T_W, f, and P_o are constants to be determined, T_S is the sidelobe contribution, which is a function of the temperature of the radiating surfaces and surface conditions, such as bare or covered by water, ice, or snow, and P_b is the interference from the beacon side tones in the radiometer pass band. Beacon interference was detected at 20.2 GHz. The waveguide components are thermally coupled to the outside air temperature. Neglecting beacon interference, this equation can be simplified to yield

$$T_B = \alpha\left(\frac{T_A + 273}{270}\right) + \beta T$$

where α, β are the simplified calibration constants and T_A is the ambient air temperature in Celsius.

The automatic calibration scheme provides the needed system stability but does not provide the estimates of α, β needed for an overall system calibration. Normally, the overall calibration would be done by using antenna tilt scans. The high far sidelobe levels of the antenna included with the ACTS propagation terminal prevented the use of this classical calibration technique. For the ACTS propagation terminal, the system calibration was established by comparing the sky brightness temperatures observed by the radiometer to those predicted theoretically based on simultaneously measured vertical profiles of atmospheric temperature and relative humidity. Only two of the measurement sites have access to vertical profile measurements obtained from radiosonde balloon ascents. For all the sites, a standard statistical prediction procedure is employed based on the use of the simultaneous meteorological measurements made at the surface (or, if the instrumentation is not working, obtained hourly from nearby National Weather Service observations). A least-squares linear regression analysis was performed using the theoretical calculations of sky brightness temperature for 108 vertical profiles measured in Norman, OK and simultaneously observed surface-temperature and water-vapor density values. The sky brightness temperature prediction procedure uses the surface values, the regression parameters, and a theoretical adjustment for changes in surface pressure. The maximum difference between the theoretical calculations and the estimates based on the regression analysis was 12 K ($\sim$ 0.2 dB attenuation) and the rms difference was less than 5 K. Long-term testing of the surface-based calibration algorithm was done at the Oklahoma site. Recent observations during cloud-free periods show less than a 3.9-K rms difference between the values estimated from surface observations and the theoretical calculations using radiosonde data.

To finish the calibration process, the sky brightness temperature estimates must be transformed to attenuation estimates. This is accomplished using the radiative transfer equation for a nonscattering atmosphere and an effective medium temperature [18]. The effective medium temperature was calculated theoretically for each of the vertical profiles employed for the regression analysis and a second regression analysis was performed to provide a statistical relationship between the theoretical medium temperature values and surface-temperature and water-vapor density. The statistically estimated effective medium temperature should be used only for clear-sky applications but, as a reasonable approximation, it is used for all situations when the attenuation is not too large. The path attenuation is obtained from

$$A = -4.34 \ln\left(\frac{T_m - T_B}{T_m - 2.74}\right)$$

where $A =$ attenuation (in dB) and $T_m =$ effective medium temperature (K).

Two sets of observations are needed to complete the calibration: one to establish the bias (or α) and the other to establish the slope (or β). The first set is obtained from observations during clear conditions when the attenuation values are low and well estimated by the clear-air attenuation predictions based on surface measurements. The second set is obtained during periods when the attenuation values are higher and the change in attenuation observed by the radiometer can be compared to the change in beacon signal level.

It is generally more convenient to compare the radiometer attenuation estimates with the calculated attenuation values obtained from the sky brightness temperature estimates than to compare measured and predicted sky temperature. The two parameters in the linear relationship, bias and slope, must still be selected but the tests can be made on the observed and predicted values of attenuation. Fig. 6 shows the relationship between radiometer measurements of attenuation and the predicted values of gaseous absorption at 20.2 GHz on March 6, 1995. Fig. 7 shows the relationship between the radiometer and beacon measurements of attenuation at 20.2 GHz on March 7, 1995.

The comparison between the attenuation estimates derived from the radiometer measurements and the gaseous absorption estimates shows a small variability, less than 0.05 dB, and larger positive excursions caused by clouds. The plotted points are for each minute of the data displayed in Fig. 2. The solid line indicates the expected results if the calibration were perfect. The dotted line is the best-estimate calibration for this day. The difference is slightly larger than 0.2 dB. The statistical uncertainty in the estimate of gaseous absorption using the surface observations and the regression parameters is 0.2 dB, where less than 0.1 dB is due to the use of the surface values and the remainder is due to the inherent error in the theoretical estimate due to humidity measurement errors. The comparison between the radiometer and gaseous absorption estimates should change by less than 0.2 dB from one day to the next.

The comparison between the radiometer and beacon estimates of attenuation (Fig. 7) is for the data displayed in Fig. 5. Most of the minute-by-minute observations lie along the 1:1 curve, indicating agreement. The larger radiometer estimates for beacon-attenuation observations of less than 0.3 dB are from the sun intrusion. The wander of the

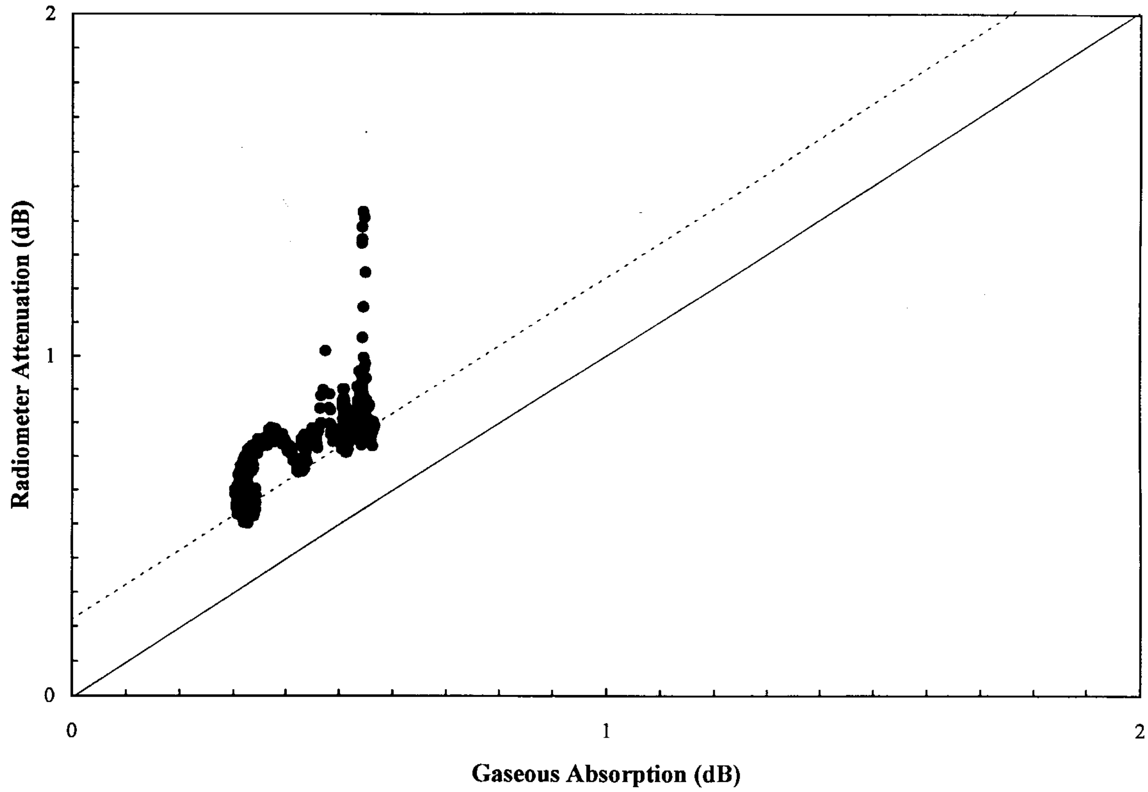

Fig. 6. Radiometer attenuation versus gaseous absorption estimates at 20.2 GHz, March 6, 1995, Norman, OK.

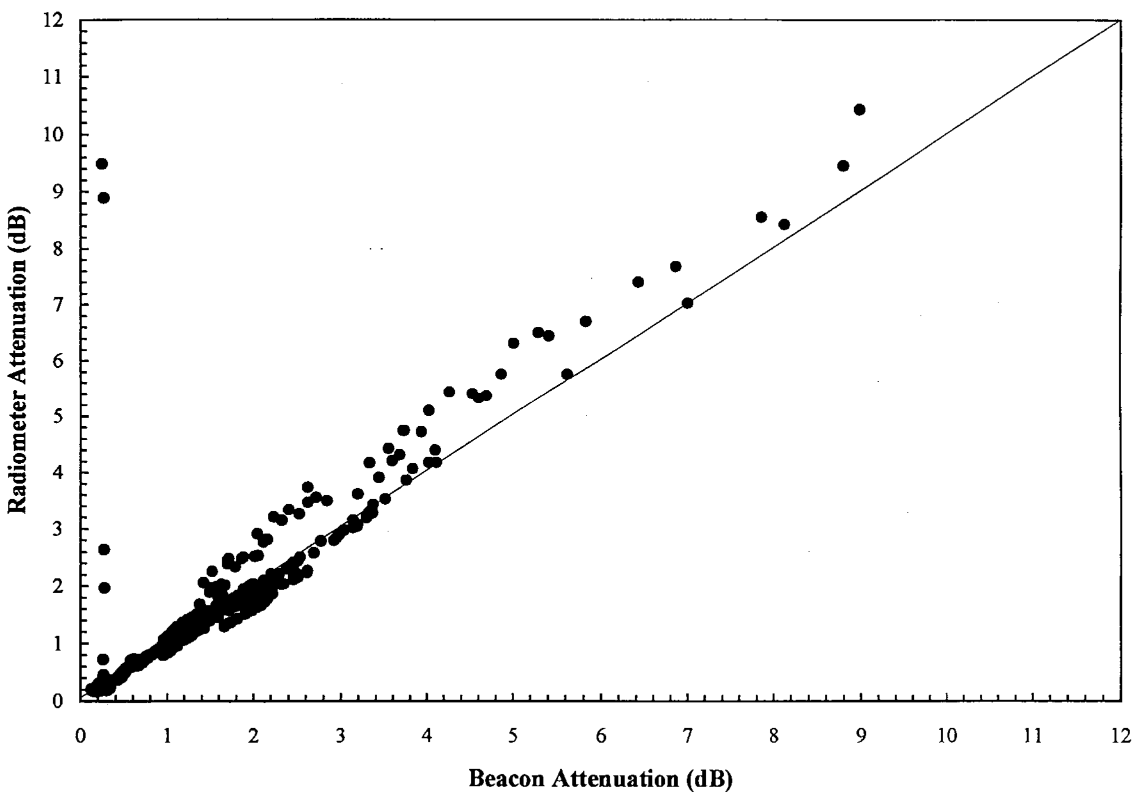

Fig. 7. Radiometer attenuation versus beacon attenuation at 20.2 GHz, March 7, 1995, Norman, OK.

points from the 1:1 curve for beacon-attenuation values of 2–9 dB are caused by attenuation by rain. In rain, the nonscattering radiative transfer equation is not exact. The location of the dominant rain scatterers are at different distances from the propagation terminal than the dominant sources of gaseous absorption, producing errors when using

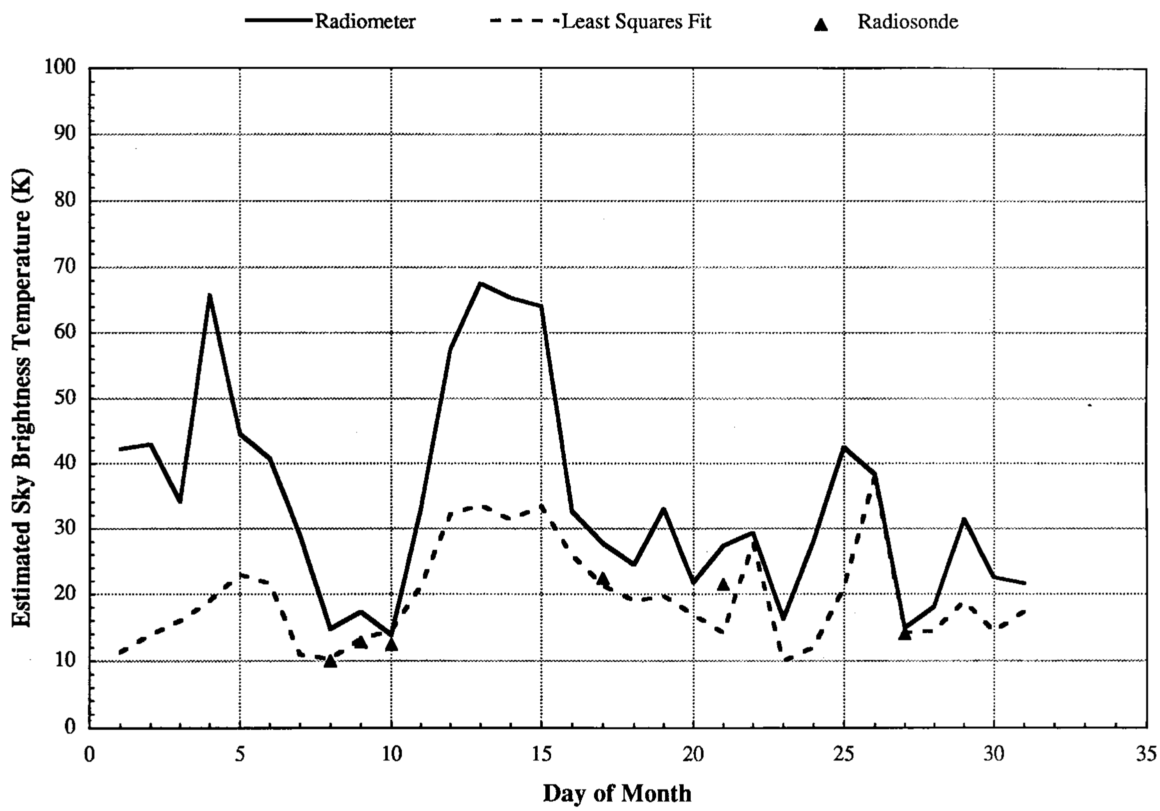

Fig. 8. Sky brightness temperature at 20.2 GHz for 12 h UT for comparison with the theoretical calculations using vertical profile data, March 1995, Norman, OK.

the effective medium temperature calculated for clear-sky conditions. With attenuation by rain, the contributions of the multiply scattered components of the radiation field from the ground or cold sky can also be significant. Adequate calibration is obtained when the majority of points in the 0–2 dB range lie along the 1:1 curve. The role of the radiometer is to provide the low attenuation reference. The calibration scheme works when the calibration errors (deviations from the 1:1 line) shown in Fig. 6 are small. Good agreement, as shown in Fig. 7, just extends the dynamic range of the values of the atmospheric parameters (surface-temperature and water-vapor density) for which the coefficients for the beacon reference level prediction scheme can be estimated without error.

The gaseous absorption estimates based on the use of the surface parameters and the regression analysis provide an approximation to the values obtained from calculations using vertical profiles. Fig. 8 presents the results of sky brightness temperature estimates at the time of the 12 h UT radiosonde balloon ascent from Norman, OK. The triangles are the results of the theoretical calculations on days when no liquid water clouds were present at the time of the balloon sounding. The solid curve is from the radiometer observations and the dashed curve is from the regression analysis based on surface data. The maximum difference between the theoretical calculations and the estimates based on the regression analysis was 11 K ($\sim$ 0.2 dB attenuation). At times without clouds, the radiometer-derived sky brightness temperature estimates averaged 3.1-K high. For both frequencies and the 0 h UT and 12 h UT radiosonde ascents, the average difference was 1.5 K and the rms difference was 3.9 K. For a comparison between the radiometer estimates and the theoretical sky noise values, the average difference was 0.3 K and the rms difference was 4.2 K. The result is a small calibration bias error of less than 0.3 K (much less than 0.1 dB). During periods with clouds or rain, the radiometer estimates must be higher than the estimated values based on surface observations and an assumption of clear-sky conditions.

A full system calibration must be performed whenever any of the antenna, waveguide, or low noise amplifier RF components are changed due to possible changes in the match between the components. Changes induced by large variations in ambient temperature may also affect the calibration. The system calibration is continuously monitored by comparing the radiometer attenuation values with the gaseous absorption estimates for the minutes of observations in each day when the standard deviation of the radiometer attenuation is less than an elevation-angle-dependent threshold value. The test on standard deviation removes time periods when significant clouds or rain occur on the path. Fig. 4 presents the minute-by-minute standard deviation values for March 7, 1995. The periods with rain and clouds are evident as intervals with varying radiometer standard deviation values between 0 and 12 h UT. After 12 h UT, the atmosphere was considered cloud-free and the results of a comparison between the gaseous absorption estimates and attenuation calculations from the radiometer

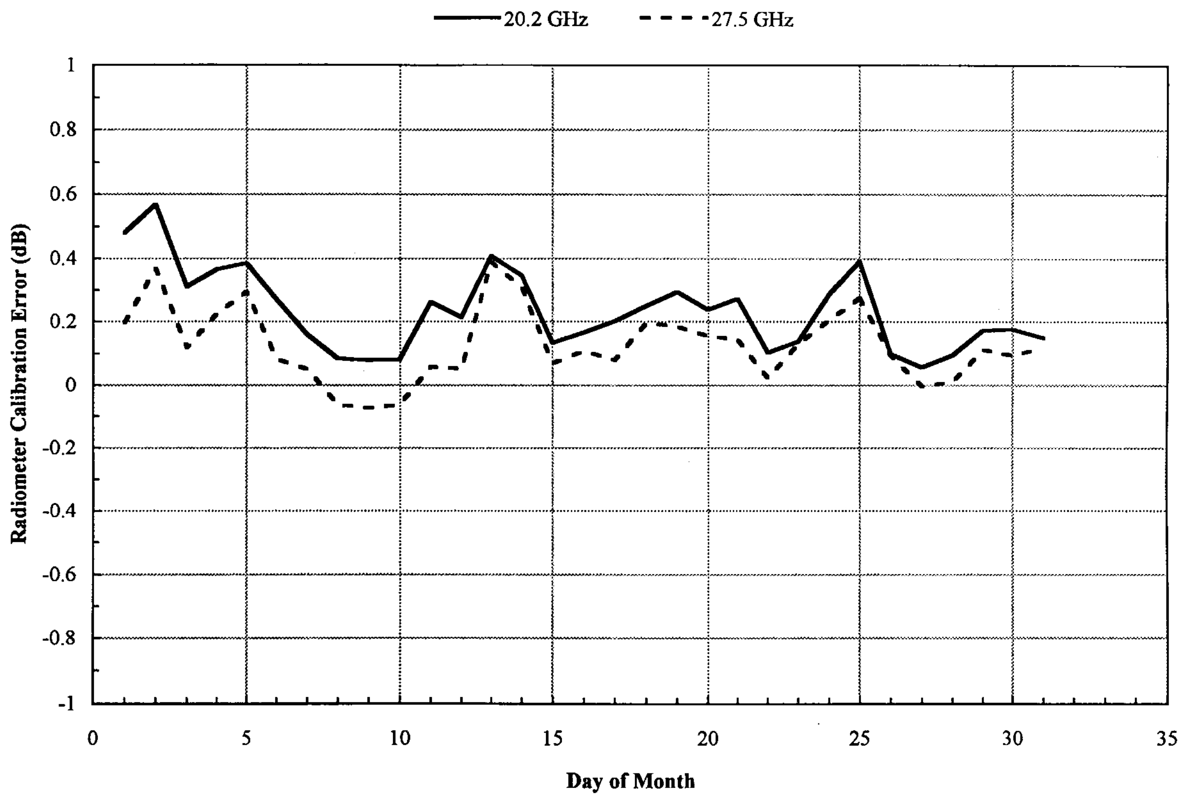

Fig. 9. Average difference between radiometer attenuation estimates and gaseous absorption estimates, March 1995, Norman, OK.

data were used to monitor system calibration. The standard deviation threshold for the Norman site was 0.005 dB, which accepted data for comparison after 12 h UT and from short intervals between 0 and 12 h UT.

The experimenters performed their own overall system calibrations. The preprocessing program provided daily and monthly summaries of the differences between the radiometer-measured attenuation values and the gaseous absorption estimates (calibration errors—Figs. 9 and 10). These data were used by the experimenters to monitor overall system calibration to determine when a new calibration must be made. They are stored in the monthly log files. Sufficient data are stored in the archives to verify the overall system calibration and to change the calibration constants if necessary.

Fig. 9 displays the average calibration errors for Norman, OK, for March 1995. The indicated average daily calibration error was less than 0.4 dB on all but two days in the month. On the two days with larger average errors, widespread cloudiness was present for most of the day and the results must be biased high due to cloud contamination. Fig. 10 displays the number of minutes used for the calculation of the average calibration error. For the first seven days of the month, no more than half of each day was used for the calculation of calibration error. The rest of the time was contaminated by significant cloudiness. Because of possible cloud contamination, the intervals with the smallest calibration errors should be used to judge the adequacy of the system calibration. Based on the receiver system design, the system calibration should only change when work is done on the system or a failure occurs in a system component. The calibration constants were not adjusted continuously to remove the small variations evident in Fig. 9.

D. Effect of a Water Coating on the Antenna

The beacon and radiometer calibration procedure maintains agreement between the beacon and radiometer attenuation estimates at values below about 4 dB and standard deviation values below 0.1 dB at high-elevation-angle sites. After calibration, the system will detect and record attenuation due to any cause. One problem mentioned above is attenuation by a thin water coating and beads of water on the antenna reflector surface, or by a thin water layer on the antenna feed horn window. The physical cause of the observed attenuation is different in each case. A water coating on the feed window must be traversed by the detected radiation. The water produces a thin transmission layer next to the dielectric layer forming the window. Water on the antenna surface produces a thin layer that moves the reflecting surface and produces attenuation in the lossy reflecting layer. Reflection from the ACTS propagation terminal antenna surface is complicated by the existence of a crinkled plastic dielectric coating over the conducting surface of the reflector, which provides a spacer separating the partially reflecting water layer and water droplets from the conducting surface. Because the plastic surface is not smooth, the antenna surface does not shed water quickly.

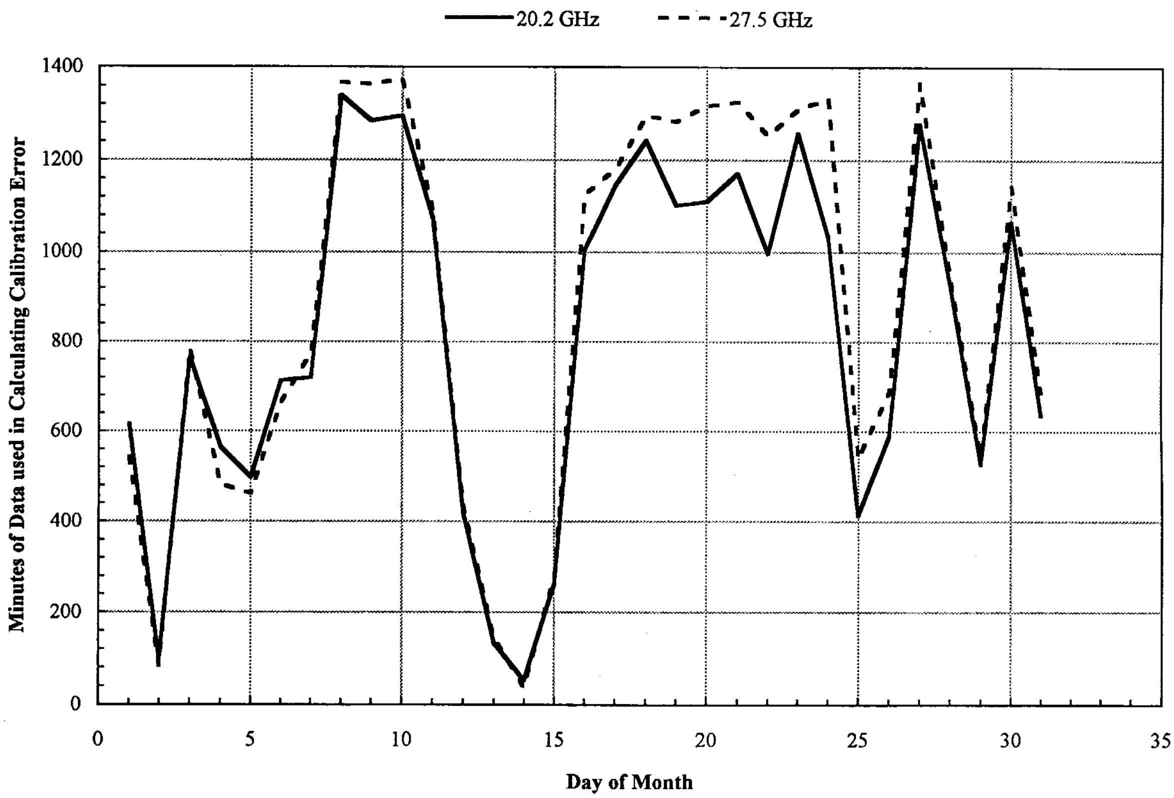

Fig. 10. Number of minutes in each day used for the calculation of the average calibration error, March 1995, Norman, OK.

Experimentally, we found that water on the reflector produced a higher attenuation than water on the feed window. Measurements displayed in Fig. 11 were made by spraying a fine mist of water onto the reflector surface. Peak attenuation values of 1.9 dB at 27.5 GHz and 1.0 dB at 20.2 GHz were obtained. The attenuation decayed slowly as the surface dried. The mist was sprayed uniformly onto the surface until the water first began to run down the surface. Only one rivulet was formed. Subsequent measurements show that values as high as 5 dB of attenuation are possible by wetting the surface continuously with a hose [19]. During periods with condensation or dew on the reflector surface, attenuation values as high as 4 dB have been observed at 27.5 GHz [20].

Both radiometer and beacon attenuation values are displayed in Fig. 11. The vertical dot dashed lines indicate three of the eight times when the radiometers were calibrated during the two-hour period. The shifts in radiometer attenuation values after the indicated calibration times are in response to corrections for drift in the radiometer system. The calibration adjustments are on the order of 0.1 dB and both positive and negative adjustments are evident. An abrupt 0.1 dB downward shift in the beacon attenuation values is evident at 27.5 GHz just before 15 h UT, with a corresponding but smaller downward shift in the 20.2-GHz attenuation values. Within the occasional 0.1-dB uncertainties in the one-minute average attenuation values, the radiometer and beacon attenuation values closely track each other. A rare moon intrusion is also evident in the radiometer output.

Spraying water on the antenna feed window produced peak attenuations of 0.2 dB at 20.2 GHz and 0.4 dB at 27.5 GHz, as shown in Fig. 12. The feed surface is considerably smaller than the reflector surface, the plane of the window surface is nearly vertical, and the surface coating sheds water. The net result was little water accumulation on the surface and rapid drying. We did the experiment twice, first with a fine mist used to generate a water coating with thickness and beading similar to the coating on the antenna producing the attenuation shown in Fig. 11 and again with as much water as we could get to accumulate on the window. The experiments were about 20 min apart. Only the second experiment produced measurable results.

The amount of water coating a surface depends upon the material, surface roughness, and exposure of the surface to aging. Both experiments reported here are for relatively new surfaces. The experiment reported in Fig. 11 was performed four months after the antenna was installed. The experiment reported in Fig. 12 was performed three months after a new feed window was installed. No special hydrophobic coating was applied to the antenna reflector but a hydrophobic coating had been applied to the feed window by the manufacturer. As a second test, an older window was subject to a similar test. The result was a maximum attenuation of 1.2 dB for an antenna installation with a much smaller elevation angle (8° versus 49°) with a feed window surface that was not vertical [21].

The wet antenna surface and wet feed surface experiments both produced attenuation values that were nearly

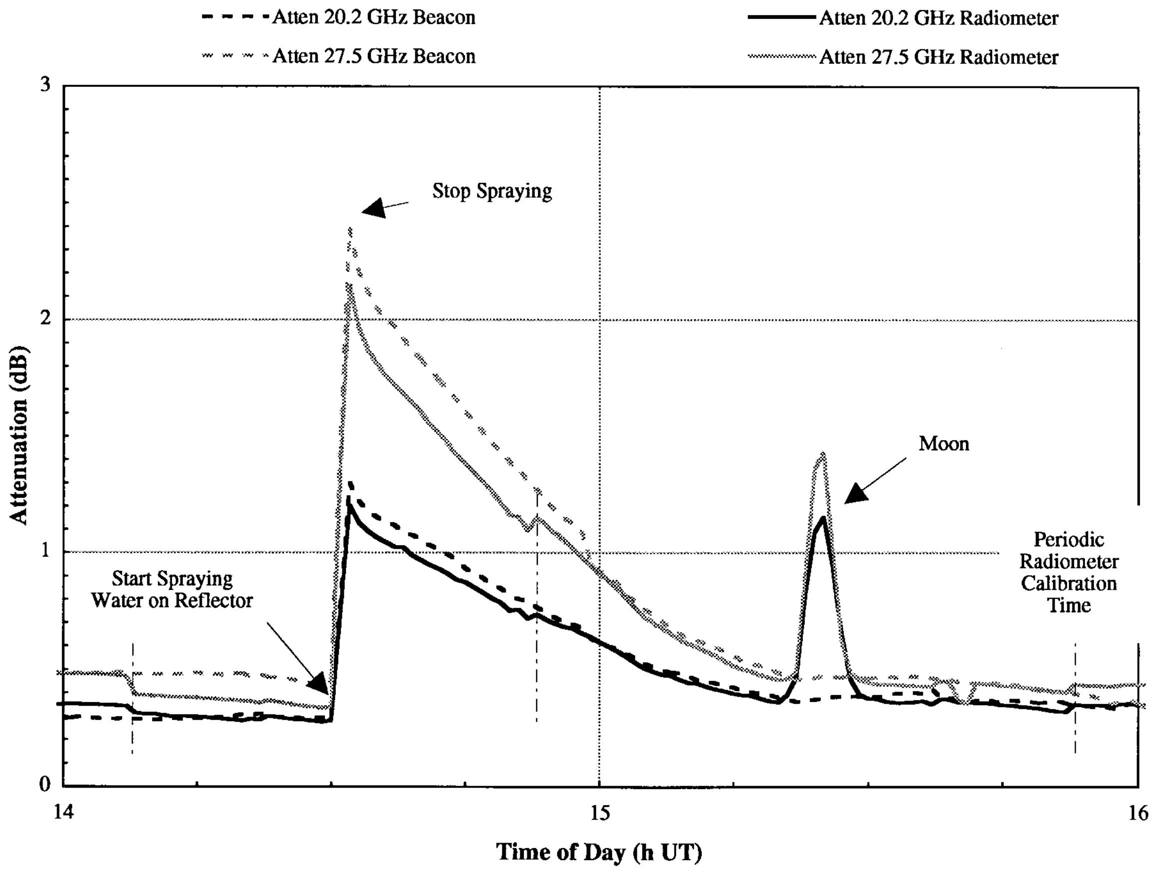

Fig. 11. Attenuation produced by spraying water on the antenna reflector, November 10, 1993, Norman, OK.

identical for the beacon signal and the radiometer estimates derived from sky brightness temperature. The result is an attenuation in addition to the path attenuation produced by rain, clouds, and gaseous absorption. No attempt was made to remove this component of the total attenuation from the observations. For the type of antenna that is used in the ACTS propagation experiment, attenuation by water on the antenna surface produces an attenuation that will affect communication system operation. This component of the total attenuation is important only when attempting to model or predict attenuation for a path. The models must take it into account. The magnitude of the effect of water on the antenna reflector surface is a function of the antenna design, and a better design should produce less of a problem.

The problem of water on antenna surfaces was considered during OPEX [5]. None of the antennas used in the OLYMPUS experiment produced attenuation values as high as those observed in ACTS due to water on the antenna surface. They reported attenuation values less than 1–2 dB in the 20–30 GHz range. The OPEX antennas were of different designs but not one of the antennas had a reflecting surface covered by a crinkled plastic surface. For the ACTS propagation experiment, the wet antenna could produce as much as 3 dB of attenuation at 20.2 GHz and 5 dB at 27.5 GHz in addition to the path attenuation during periods of heavy rain.

V. Data Preparation and Archival

A. Preprocessing

The preprocessing program does the following:

1) reads the unprocessed data;
2) performs radiometer calibration;
3) predicts the beacon reference levels and accumulates the sums necessary to determine the coefficients in the reference level prediction model for the next hour and for the next day;
4) corrects the 20-GHz beacon observations by removing the ranging ones;
5) generates the one-minute average and standard deviation values for output to daily summary files;
6) tabulates histograms for beacon and radiometer attenuation levels, beacon fade durations, and interfade intervals;
7) writes the preprocessed data files;
8) writes auxiliary data to a log file and other files needed for the reconstruction of the unprocessed data from the preprocessed data.

The calibrated preprocessed data files are produced for public use. Auxiliary data files are also recorded to provide the calibration and reference level generation data needed to go from an attenuation estimate back to the unprocessed

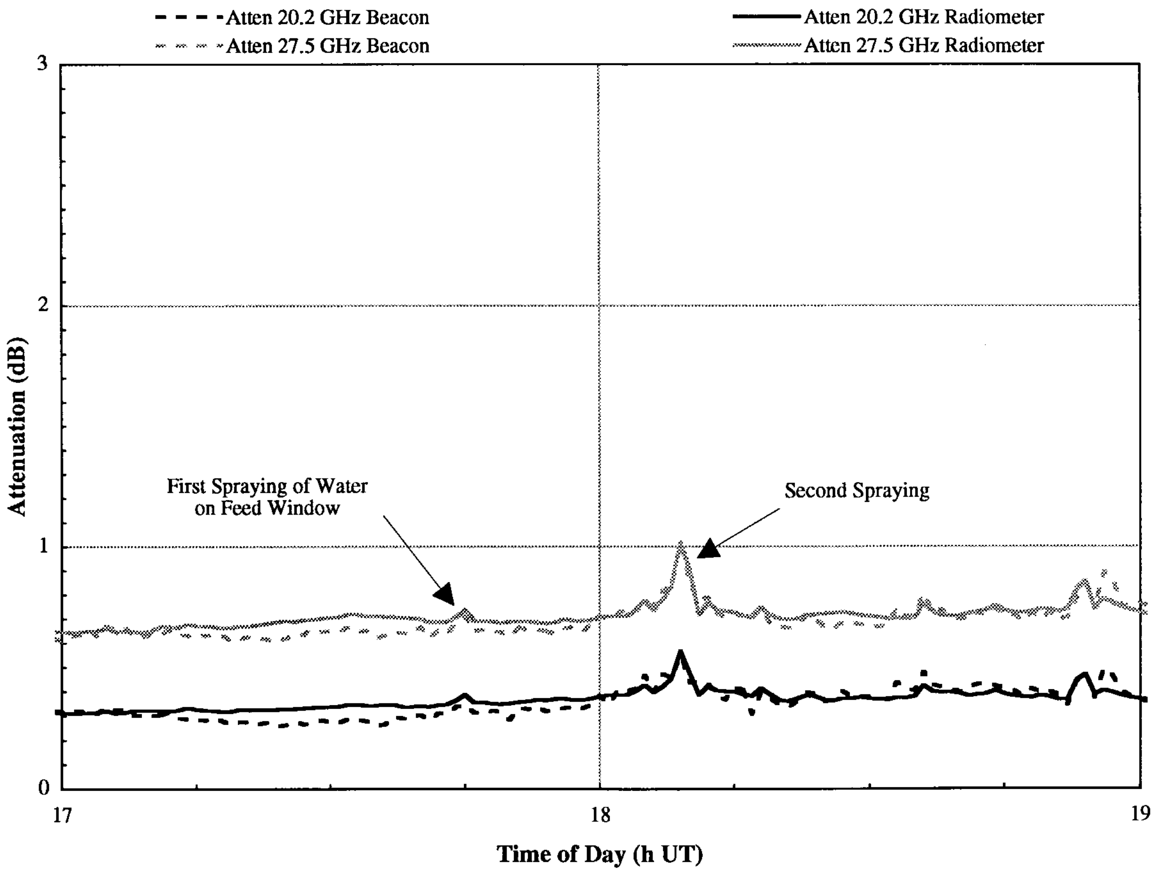

Fig. 12. Attenuation produced by spraying water on the antenna feed window, October 15, 1996, Norman, OK.

beacon signal level and radiometer output voltage. The need for the auxiliary files is to ensure that no information is lost in data preprocessing.

The histogram and auxiliary data files contain all the information for a calendar month. The histogram file contains:

1) the attenuation relative to free space distribution estimates for one-second and one-minute integration times for the beacon and radiometer observations;
2) the fade duration and interfade interval data for the one-second integration time series of attenuation relative to free space;
3) the one-minute integration time beacon attenuation relative to clear-sky conditions (corrected for gaseous absorption);
4) the one-minute average sky brightness temperature estimates;
5) the standard deviation estimates for the one-second integration time beacon and radiometer attenuation values relative to free space observed in a minute;
6) the one-minute rain-rate estimates from collocated tipping bucket or capacitor rain gauges.

The auxiliary files include ranging tone times and signal strength changes; log files that contain information about radiometer calibration errors, receiver performance, and experimenter-prepared good and bad data time intervals; surface meteorological data for times when the surface observations from the propagation terminal are not correct; and the model parameters used for reference-level estimation.

Several different data preprocessing modes are possible. They work for input of the unprocessed data or for previously preprocessed data. The normal mode generates the summary output data described above. A second preprocessing mode provides a summary output containing all the status parameters recorded in the unprocessed data and also stored in the preprocessed data. This mode is for receiver diagnostic work to detect and determine the possible causes of receiver operation problems. Another mode generates a summary output file for every second of observation between specified start and stop times. These processing modes can be used to verify or change the receiver calibration constants.

Histograms can be generated by three different program modes: the normal mode, which uses the same time base for the tabulation of the histograms for different frequencies, beacon channels, and radiometer channels; the single frequency mode, which uses different time bases for the two frequencies but the same time base for the beacon and radiometer channels at a single frequency; and the independent mode, with different time bases for each frequency and receiver channel. In the normal mode, the results can be used for frequency scaling. These modes can be selected whenever the preprocessing program is run to generate a histogram output. The different modes are available to provide output when one of the receiver channels is not functioning properly.

B. Data Archival

The unprocessed and preprocessed data are collected by the experimenters and sent to the University of Texas for archival [12]. There, the data are catalogued subject to quality-control checks, compressed to minimize storage, and stored until requested by the public. The compressed preprocessed data are available on CD-ROM.

VI. Conclusion

The results from the first two years of the ACTS propagation experiment are available from the archives or from the papers in this special issue of the Proceedings. The continuous calibration monitoring assures data that are within the 0.5-dB measurement error specifications of the experiment design. The log files provide a continuous record of the availability of the propagation terminal for measurements that document possible errors in sampling the attenuation statistics.

The preprocessing program provides the minimum output from the experiment, attenuation, fade duration, interfade interval, sky brightness temperature, and rain-rate histograms. Two attenuation outputs are available: 1) total attenuation or attenuation relative to free space and 2) rain attenuation or attenuation relative to clear-sky conditions. The format of the recorded data provides easy access to the statistics on a monthly basis. Worst-month statistics are readily available. The continued development of propagation models will require access to the monthly statistics of attenuation and auxiliary parameters such as rain rate, surface temperature, and surface water-vapor density. The ACTS propagation experiment is unique in the amount of data it has collected and is making available to the propagation community for continued analysis.

References

[1] F. Davarian, "Ka-band propagation research using ACTS," *Int. J. Satell. Commun.*, vol. 14, no. 3, pp. 267–282, 1996.

[2] P. Gargione, R. Acosta, T. Coney, and R. Krawozyk, "Advanced communications technology satellite (ACTS): Design and on-orbit performance measurements," *Int. J. Satell. Commun.*, vol. 14, no. 3, pp. 133–160, 1996.

[3] "Acquisition, presentation and analysis of data in studies of tropospheric propagation," Recommendation PN.311-7, *ITU-R Recommendations*, PN Series, ITU, Geneva, 1994.

[4] D. C. Cox and H. W. Arnold, "Results from the 19- and 28-GHz COMSTAR satellite propagation experiments at Crawford Hill," *Proc. IEEE*, vol. 70, pp. 458–488, May 1982.

[5] J. P. V. Poiares Baptista, *Reference Book on Attenuation Measurement and Prediction*, vol. 1. Noordwijk, The Netherlands: OPEX, ESA-WPP 083, 1994.

[6] R. K. Crane, *Electromagnetic Wave Propagation Through Rain.* New York: Wiley, Interscience, 1996, p. 9.

[7] A. W. Dissanayake, "Application of open-loop uplink power control in Ka-band satellite links," this issue, pp. 959–969.

[8] E. H. Satorius and L. H. Tong, "Analysis of a rain compensation algorithm for K/Ka-band communications," *Int. J. Satell. Commun.*, vol. 14, no. 3, p. 297, 1996.

[9] R. K. Crane and H-C Shieh, "A two-component rain model for the prediction of site diversity improvement performance," *Radio Sci.*, vol. 24, no. 6, pp. 641–655, 1989.

[10] J. Goldhirsh, B. H. Musiani, A. W. Dissanayake, and K.-T. Lin, "Three-site space-diversity experiment at 20 GHz using ACTS in the eastern United States," this issue, pp. 970–980.

[11] W. Stutzman, T. Pratt, C. Nunnally, R. Nealy, W. Remaklus, A. Predoehl, and A. Gaff, "ACTS propagation terminal, hardware description report," Virginia Polytechnic Institute and State University, Virginia Tech Rep. EE SATCOM 93-3, Blacksburg VA, 1993.

[12] W. J. Vogel, "ACTS propagation experiment data archives," Electrical Engineering Research Laboratory, University of Texas, Austin, 1996.

[13] R. K. Crane, "Estimating risk for earth-satellite attenuation prediction," *Proc. IEEE*, vol. 81, pp. 905–912, June 1993.

[14] ——, University of Oklahoma Propagation Experiment Archives, School of Meteorology, University of Oklahoma, Norman.

[15] "Propagation data and prediction methods required for earth-space telecommunication systems," Recommendation ITU-R P.618-4, *ITU-R Recommendations*, P-Series Fascicle, ITU, Geneva, 1996.

[16] A. W. Dissanayake, J. E. Allnutt, and F. Haidara, "A prediction model that combines rain attenuation and other impairments along earth-space paths," *IEEE Trans. Antennas Propagat.*, submitted for publication.

[17] R. K. Crane, "Prediction of attenuation by rain," *IEEE Trans. Commun.*, vol. COMM-28, pp. 1717–1733, Sept. 1980.

[18] ——, "Propagation phenomena affecting satellite communication systems operating in the centimeter and millimeter wavelength bands," *Proc. IEEE*, vol. 59, pp. 173–188, 1971.

[19] V. N. Bringi and J. Beaver, "Ka-band propagation studies using the ACTS propagation terminal and the CSU-CHILL multiparameter radar," in *Proc. 20th NASA Propagation Experimenters Meeting (NAPEX XX)*, Jet Propulsion Lab., Pasadena, CA, 1996, pp. 85–112.

[20] R. K. Crane and A. W. Dissanayake, "ACTS propagation experiment: Attenuation distribution observations and prediction model comparisons," this issue, pp. 879–892.

[21] C. E. Mayer, personal communication, Univ. Alaska, Fairbanks, Oct. 1996.

Robert K. Crane (Fellow, IEEE) received the B.S., M.S., and Ph.D. degrees in electrical engineering from Worcester Polytechnic Institute, MA.

In 1981–1992, he was Research Professor of Engineering at the Thayer School of Engineering, Dartmouth College. In 1976–1981, he was Deputy Division Manager and Division Senior Scientist at Environmental Research and Technology, Inc. In 1964–1976, he was a staff member in MIT's Lincoln Laboratory. He currently is Professor of Meteorology and Professor of Electrical Engineering at the University of Oklahoma, Norman. He has spent his research career conducting studies in electromagnetic wave propagation through the atmosphere and in the remote sensing of precipitation via radio and radar techniques.

Dr. Crane is a member of the American Meteorological Society and the American Geophysical Union. He has been active in the work of Commission F of the International Union of Radio Science (URSI) and in the United States National Committee for URSI. He has also been active in the work of Study Group 3 of the radiocommunications sector of the International Telecommunications Union.

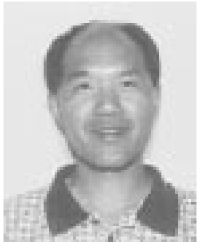

Xuhe Wang received the B.S. degree in laser physics from Southeast University, Nanjing, P.R. China, in 1984, and the M.S. degree in meteorology from the University of Oklahoma, Norman, in 1996. He is currently working toward the M.S. degree in computer science at the University of Oklahoma.

Since May 1993, he has been a Research Assistant for R. K. Crane in the ACTS propagation experiments for central Oklahoma. His research interests are in the areas of rain attenuation and tropospheric scintillation effects on Ka-band satellite communication.

D. B. Westenhaver received the B.S. degree in applied physics from Auburn University, AL, and did graduate work at the University of New Mexico, Las Cruces.

He started his career with EG&G, where he worked in multiple areas of electromagnetic pulse propagation, wideband telemetry systems, dielectric waveguide research, and reverse engineering. Later, he was with Scientific-Atlanta, where he worked on all aspects of antenna systems and data-collection systems, specializing in Servo and Tracking Systems. He designed, developed, and coded the Operator Control Station and System Controller containing features such as satellite predictions, satellite pass scheduling, and built-in system testing. In 1990, he founded Westenhaver Wizard Works, Inc., Stone Mountain, GA, a scientific and systems consulting firm. Since 1992, he has provided system engineering support and hardware and software upgrades for the ACTS propagation terminals.

Wolfhard J. Vogel (Fellow, IEEE) studied electrical engineering at the Technical University of Berlin, Germany. He obtained a scholarship to study at the University of Texas at Austin, where he received the M.S.E.E. and Ph.D. degrees in electrical engineering.

He is currently Associate Director of the Electrical Engineering Research Laboratory of The University of Texas at Austin. He has authored numerous publications in the area of satellite-earth wave propagation research, emphasizing rain attenuation and depolarization effects and fading due to shadowing and multipath for land-mobile and personal satellite communications from UHF to K-band. He is currently engaged in studies characterizing propagation phenomena pertinent to satellite sound broadcasting, low-earth-orbit satellite communication systems, and smart antennas.

Dr. Vogel is Chairman for Commission F of the U.S. National Committee of the International Union of Radio Science (Wave Propagation and Remote Sensing) and chairs the IEEE Standards Committee for Propagation.